International Endodontic Journal

doi:10.1111/j.1365-2591.2010.01767.x

The effect of root canal taper on the irrigant flow: evaluation using an unsteady Computational Fluid Dynamics model

C. Boutsioukis[1,2], C. Gogos[1], B. Verhaagen[3], M. Versluis[3], E. Kastrinakis[4] & L. W. M. van der Sluis[2]

[1]Department of Endodontology, Dental School, Aristotle University of Thessaloniki, Thessaloniki, Greece; [2]Department of Cariology, Endodontology, Pedodontology, Academic Centre for Dentistry Amsterdam (ACTA), Amsterdam, The Netherlands; [3]Physics of Fluids Group, Faculty of Science and Technology, and Research Institute for Biomedical Technology and Technical Medicine MIRA, University of Twente, Enschede, The Netherlands; and [4]Chemical Engineering Department, School of Engineering, Aristotle University of Thessaloniki, Thessaloniki, Greece

Abstract

Boutsioukis C, Gogos C, Verhaagen B, Versluis M, Kastrinakis E, van der Sluis LWM. The effect of root canal taper on the irrigant flow: evaluation using an unsteady Computational Fluid Dynamics model. *International Endodontic Journal*, **43**, 909–916, 2010.

Aim To evaluate the effect of root canal taper on irrigant flow inside a prepared root canal during final irrigation with a syringe and two types of needles, using a Computational Fluid Dynamics (CFD) model.

Methodology A validated CFD model was used to simulate irrigant flow from either a side-vented or a flat 30G needle positioned inside size 30, .02 taper, 30, .04, 30, .06, ProTaper F3 or size 60, .02 taper root canals, at 3 mm short of working length (WL). Velocity, pressure and shear stress in the root canal were evaluated.

Results The side-vented needle could not achieve irrigant replacement to the WL in any of the cases. Significant irrigant replacement was evident further than 2 mm apically to the tip of the flat needle in the size 30, .06 taper, F3 and size 60, .02 taper canal. A wider distribution of wall shear stress was noted as the canal taper increased but the maximum shear stress decreased. The flat needle led to higher mean pressure at the apical foramen. Both needles showed a similar gradual decrease in apical pressure as the taper increased, but the least pressure was calculated in the size 60, .02 taper canal.

Conclusions An increase in root canal taper improved irrigant replacement and wall shear stress whilst reducing the risk for irrigant extrusion. Irrigant flow in a minimally tapered root canal with a large apical preparation size also improved irrigant replacement and wall shear stress and reduced the risk for irrigant extrusion, compared to the tapered root canals with a smaller apical preparation size.

Keywords: Computational Fluid Dynamics, irrigation, needle, root canal taper.

Received 5 February 2010; accepted 1 May 2010

Introduction

The geometrical complexity of the root canal system is considered a limiting factor for the procedures used during root canal treatment (Ørstavik *et al.* 2004). Elimination of bacteria, removal of tissue remnants and debridement cannot be accomplished solely by mechanical instrumentation (Gulabivala *et al.* 2005). Thus, irrigation with antibacterial solutions is performed as complement to mechanical preparation (Haapasalo *et al.* 2005).

The performance of irrigation depends largely on the ability of the irrigant to penetrate the full extent of the root canal system (Salzgeber & Brilliant 1977, Druttman & Stock 1989). Irrigant penetration is influenced by the original anatomy of the root canal

Correspondence: Christos Boutsioukis, 29, Kimis St, 551 33 Thessaloniki, Greece (Tel.: +302310427813; fax: +302310 999639; e-mail: chb@dent.auth.gr).

system as well as the final shape created through mechanical preparation (Ram 1977, Chow 1983, Kahn *et al.* 1995, Gulabivala *et al.* 2005). It has been reported that increasing the taper of the root canal might result in improved debridement during irrigation (Albrecht *et al.* 2004). However, this conclusion reflected the combined effect of increased canal taper and positioning of the needle closer to working length (WL) (Albrecht *et al.* 2004). On the other hand, it has also been reported that there is no significant difference between tapered and minimally tapered root canals in terms of antimicrobial efficacy of both syringe irrigation and apical negative pressure irrigation (Hockett *et al.* 2008).

Previous studies have not provided sufficient data on the flow pattern developed in the root canal, which is the cause of debridement and irrigant replacement, and whether the flow is affected by changes in root canal geometry. Hence, current understanding of the influence of canal geometry on the flow is largely based upon speculation (Ram 1977, Abou-Rass & Piccinino 1982, Chow 1983, Druttman & Stock 1989, Sedgley *et al.* 2005, Zehnder 2006).

A Computational Fluid Dynamics (CFD) model was recently applied to the study of root canal irrigation (Boutsioukis *et al.* 2009). A similar approach has also been reported (Gao *et al.* 2009). The original model was subsequently validated by comparison with experimental high-speed imaging data (Boutsioukis *et al.* 2010a) and used to evaluate the effect of various factors, such as needle tip design (Boutsioukis *et al.* 2010b) and preparation size (Boutsioukis *et al.* 2010c), on the flow. In these previous studies, the taper of the root canal was 6%.

The aim of this study was to evaluate the effect of root canal taper on the irrigant flow inside a prepared root canal during final irrigation with a syringe and two different needle types using the validated CFD model.

Materials and methods

The root canal was simulated as a geometrical frustum of a cone (the portion of a cone which lies between two parallel planes perpendicular to the cone axis). The length of the root canal was 19 mm. Five different root canal shapes were modelled. In the first three cases, the diameter at the most apical point was 0.30 mm (ISO size 30), and the taper of the root canal was 2%, 4% and 6%, respectively. The fourth case was simulated using the shape of the ProTaper F3 instrument (Dentsply Tulsa Dental, York, PA, USA) as a reference. The diameter at the most apical point was 0.30 mm (ISO size 30), and the taper of the root canal was 9% in the apical 3 mm of the canal and then it decreased gradually. The final canal shape was based on data provided by the manufacturer (Dentsply Tulsa Dental Specialties 2009) and on computer image analysis of photos obtained through Stereoscopic Microscope, with AutoCAD 2006 software (AutoDesk, San Rafael, CA, USA). In the fifth case, the diameter at the most apical point was 0.6 mm (ISO size 60), and the taper of the root canal was 2%. The diameter at the canal orifice was 0.68, 1.06, 1.44, 1.21, 0.98 mm, respectively (Fig. 1).

The apical anatomy of the root canal was also simulated as an inverted frustum of a cone with a length of 0.5 mm connected to the original frustum (Fig. 1). The diameter of the apical constriction was set to three ISO sizes smaller than the apical preparation, namely 0.15 mm for the ISO 30 cases and 0.45 mm for the ISO 60 case. The diameter of the apical foramen was set to 0.05 mm larger than the apical constriction. The apical root canal anatomy was modelled to simulate the effect of a patency file used during root canal preparation. The apical foramen was simulated as a rigid and impermeable wall.

Two different needle types, a side-vented and a flat needle, were modelled using commercially available 30G needles as references, similarly to a previous study (Boutsioukis *et al.* 2010b). The external and internal diameter and the length of the needles were standardized (D_{ext} = 320 μm, D_{int} = 196 μm, l = 31 mm, respectively). The needles were fixed and centred within the canal, at 3 mm short of WL.

The pre-processor software Gambit 2.4 (Fluent Inc., Lebanon, NH, USA) was used to build the 3-D geometry and the mesh. A hexahedral mesh was constructed and refined near the walls and in the areas where high gradients of velocity were anticipated, such as near the needle outlet. A grid-independency check was performed to determine the minimum number of computational cells required for a grid-independent flow simulation and ensure reasonable use of computational resources. The final meshes consisted of 477 000–783 000 cells (mean cell volume 0.7–2.1×10^{-5} mm^3) depending on needle type and shape of the root canal.

No-slip boundary conditions were imposed to the walls of the root canal and of the needles, under the hypothesis of rigid, smooth and impermeable walls. The fluid flowed into the simulated domain through the

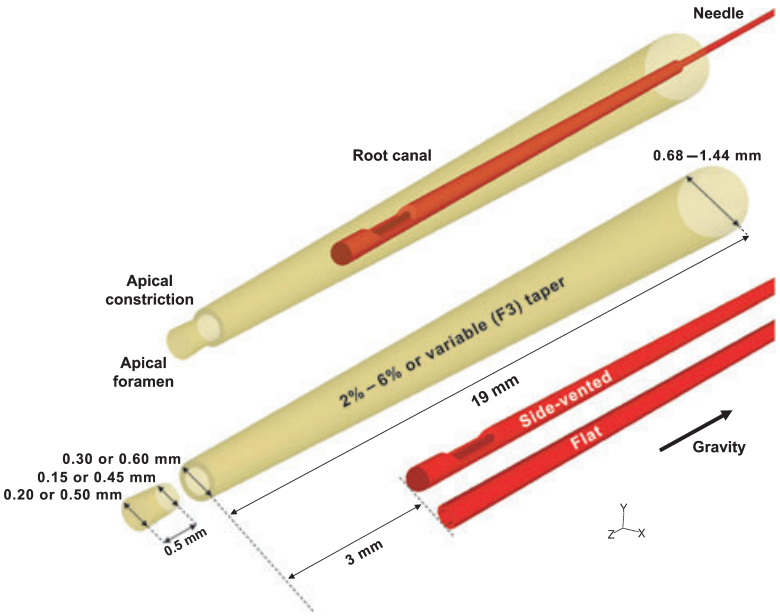

Figure 1 Geometrical characteristics of the Computational Fluid Dynamics model used.

needle inlet and out of the domain through the root canal orifice, where atmospheric pressure was imposed. The canal and needle were assumed to be completely filled with irrigant. A velocity inlet boundary condition was selected for the inlet of the needle. A flat velocity profile with a constant axial velocity of 8.6 m s^{-1} was imposed at the inlet, which is consistent with a clinically realistic irrigant flow rate of 0.26 mL s^{-1} through a 30G needle (Boutsioukis *et al.* 2007a). The irrigant, sodium hypochlorite 1% aqueous solution, was modelled as an incompressible, Newtonian fluid, an assumption that is generally accepted for pure water and sparse aqueous solutions (Tilton 1999), with density $\rho = 1.04$ g cm^{-3} and viscosity $\mu = 0.99 \times 10^{-3}$ Pa·s (Guerisoli *et al.* 1998). Gravity was included in the flow field in the direction of the negative z axis.

The commercial CFD code FLUENT 6.3 (Fluent Inc) was used to set up and solve the problem and to analyse the results. The Navier-Stokes equations which describe the time-dependent, three-dimensional, incompressible flow were solved by an implicit iterative solver. The numerical solution method uses a finite volume approach. An unsteady isothermal flow was assumed; steady-state solutions were obtained first and were used as initial conditions for the unsteady simulations, to avoid transient effects. No turbulence model was used, as the flow under these conditions was expected to be laminar (Boutsioukis *et al.* 2009, 2010a). All transport equations were discretized to be at least second-order accurate. A time-step of 10^{-6} s was used throughout the calculations, which were carried out for a real flow time of 50 ms for each needle type and position. The convergence criterion for the maximum scaled residuals was set at 10^{-4}. Pressure, velocity and vorticity in selected areas of the flow domain were also monitored to ensure adequate convergence in every time-step. Computations were carried out in a computer cluster [45 dual core AMD Opteron 270 processors (Advanced Micro Devices, Sunnyvale, CA, USA)] running 64-bit SUSE Linux 10.1 (kernel version 2.6.16).

A series of computations for five different cases for each of the two needle types were performed; the flow fields computed were compared in terms of flow pattern, velocity magnitude, shear stress and apical pressure. Lagrangian particle tracking was performed as a post-processing operation, in which the routes of massless particles were tracked throughout the flow domain after release from the inlet of the needles.

Results

An unsteady (non-stationary) flow was identified in all cases, regardless of needle type or root canal taper. The time-averaged flow pattern in the apical part of the canal presented slight differences amongst the various

cases studied, for each needle type (Fig. 2) and was similar to a previous report (Boutsioukis *et al.* 2010b).

The side-vented needle could not achieve any significant irrigant replacement apically to its tip in a size 30, .02 taper root canal, as indicated by the distribution of the axial *z*-component of irrigant velocity in the apical part of the root canal (Fig. 3). Irrigant replacement was gradually improved in the size 30, .04 taper, 30, .06 and F3 canal shapes and the most efficient replacement, up to 2 mm apically to the tip of the needle, was noted in the size 60, .02 taper canal. The flat needle led to more extensive irrigant replacement in all cases, compared to the side-vented needle. Significant irrigant replacement was evident more than 1 mm apically to the needle tip in the size 30, .02 taper canal. Irrigant replacement was also gradually improved in the size 30, .04 taper, 30, .06 and F3 canals and the most efficient replacement, up to WL, was noted in the size 60, .02 taper canal. Irrigant flow coronally to the outlet (reverse flow) showed complete replacement in these parts of the canal irrespective of needle type or preparation size, although the magnitude of the velocity varied between cases.

The shear stress pattern on the canal wall presented differences according to canal shape and needle type (Fig. 4). A maximum shear stress of almost 11 000 N m^{-2} was concentrated around the needle tip in the size 30, .02 taper root canal for both needle

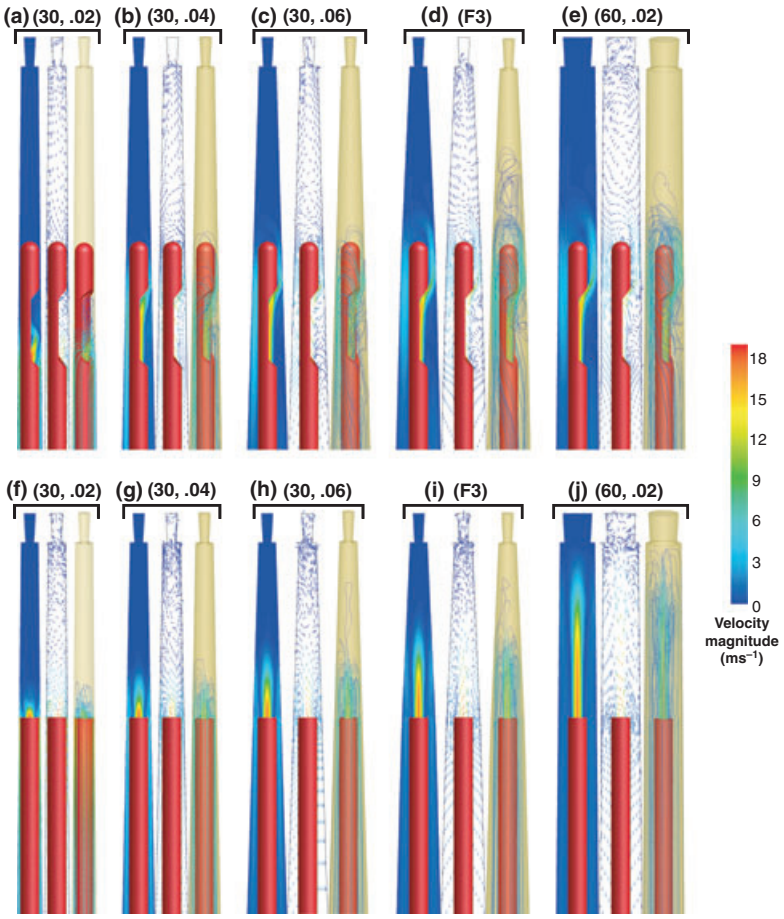

Figure 2 Triads of time-averaged contours of velocity magnitude (left) and vectors (middle) along the *z*–*y* plane in the apical part of the root canal, and streamlines indicating the route of massless particles released downstream from the needle inlet and coloured according to time-averaged velocity magnitude (right). Particle trajectories provide visualization of the main fresh irrigant flow in three dimensions. The size and position of the vortices (flow structures where the fluid is rotating) apically to the side-vented needle varied (a–e). In the size 30, .02 taper canal (a) hardly any flow could be identified apically. The extent of the jet apically to the tip of the flat needle increased from case (f) to case (j) (f–j). Needles are coloured in red.

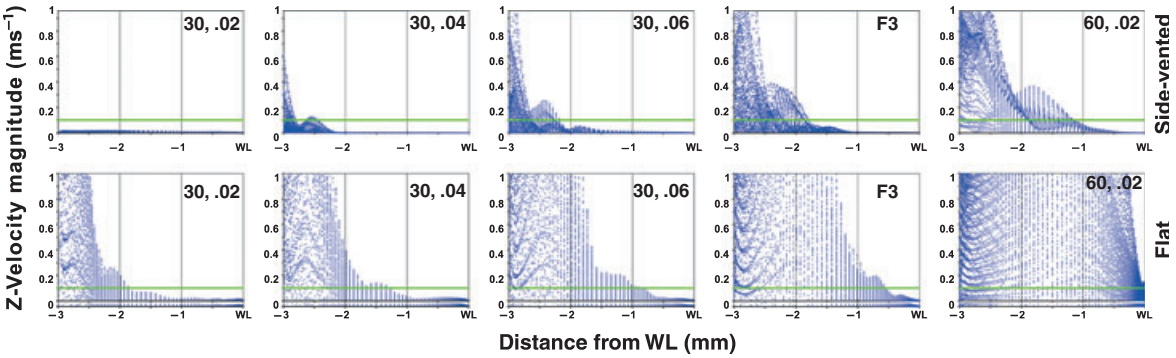

Figure 3 Distribution of the axial *z*-component of time-averaged irrigant velocity in the apical part of the canal as a function of distance from working length (WL), for the side-vented (top) and the flat needle (bottom). The needle is positioned at 3 mm short of WL. The scale of the vertical axis has been adjusted to 0–1 m s^{-1} to highlight differences in the area apically to the needle tips. Velocities higher than 0.1 m s^{-1} (horizontal green line) were considered clinically significant for adequate irrigant replacement.

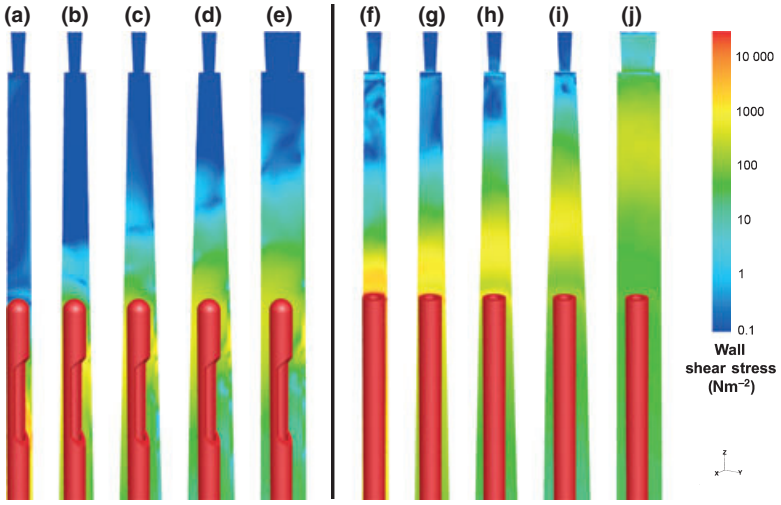

Figure 4 Time-averaged distribution of shear stress on the root canal wall for the side-vented (a–e) and flat needle (f–j) in size 30, .02 taper, 30, .04, 30, .06, ProTaper F3 and size 60, .02 taper root canals, respectively. A logarithmic colour map was used to highlight the main differences. Only half of the root canal wall is presented to allow simultaneous evaluation of the needle position. Needles are coloured in red.

types, which coincided with the maximum velocity area (Fig. 2a,f). Extremely low shear stress occurred apically to the tip of the side-vented needle in the size 30, .02 taper canal (Fig. 4a). As the taper of the root canal increased, the region apically to the tip of the needle affected by high shear stress gradually extended towards the apex, although maximum shear stress decreased. A similar effect was noted for the flat needle. The area affected by high shear stress always surrounded the tip of the side-vented needle with maximum shear stresses concentrated on the wall facing the needle outlet (Fig. 4a–e). For the flat needle, high shear stress was identified apically to its tip and equally distributed circumferentially (Fig. 4f–j). For both needle types, the area affected by high shear stress was the largest in the size 60, .02 taper canal.

The time-averaged pressure developed at the apical foramen differed amongst the various cases and needle types (Fig. 5). In all cases, the flat needle led to higher mean pressure at the apical foramen than the side-vented needle, up to 417.4 ± 3.3 kPa in the size 30, .02 taper root canal. The side-vented needles presented significantly lower mean apical pressure, with maximum of 126.3 ± 1.9 kPa in the size 30, .02 taper root

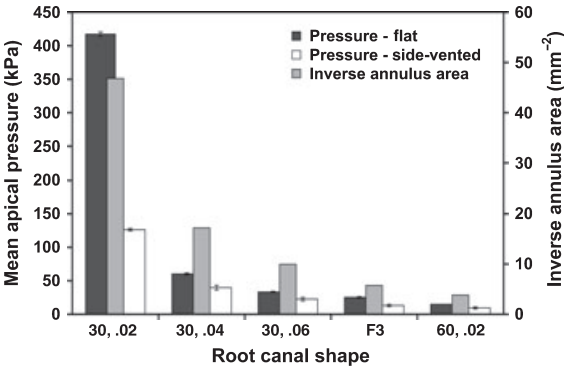

Figure 5 Time-averaged irrigant pressure at the apical foramen developed by the side-vented and the flat needle, and inverse annulus area available between the needle and the root canal wall at the tip of the needle, 3 mm short of working length, calculated according to equations 1 and 2, for the five cases studied. The decrease in the inverse annulus area from sizes 30, .02 taper to 60, .02 is very similar to the decrease in the mean apical pressure. Pressure data are shown as mean ± standard deviation.

canal. Apical pressures showed a similar gradual decrease from sizes 30, .02 taper to 60, .02 for both needle types.

Discussion

The purpose of this study was to investigate the effect of root canal taper on irrigant flow inside a prepared root canal. To evaluate such an effect, five different canal shapes were studied. In the first three, the apical size was ISO 30 and the taper of the root canal was gradually increased (2%, 4% and 6%). The fourth case simulated a root canal with a variable taper, also with an apical size of ISO 30, but the taper of the root canal was adjusted using the ProTaper F3 instrument (Dentsply Tulsa Dental) as a reference. The fifth case (size 60, 2% taper) was selected to compare irrigant flow in tapered root canals to the one developed in a minimally tapered root canal. Two representative needle types were used in each of the five root canals simulated, to evaluate the effect of canal taper on irrigant flow and allow comparison with previous studies. Both needles were positioned at 3 mm short of WL to facilitate standardization between different cases studied, as it was not possible to position the needles closer to WL in the size 30, .02 taper canal.

The relevance of the *z*-velocity magnitude, the shear stress and the apical pressure to irrigation has been analysed previously (Boutsioukis *et al.* 2010b). In this study, an increase in the taper of the root canal was shown to have a direct effect on irrigant flow, resulting in more efficient replacement and debridement in the apical part of the root canal, apart from allowing penetration of the needle closer to WL (Albrecht *et al.* 2004). These findings corroborate previous studies (Albrecht *et al.* 2004, Huang *et al.* 2008). However, standardization of needle insertion depth is a prerequisite for a detailed comparison with the results of this study, because the effect of needle depth on irrigant flow has also been reported to be significant (Sedgley *et al.* 2005, Hsieh *et al.* 2007).

No significant difference in the antimicrobial efficacy of syringe irrigation in tapered and minimally tapered root canals has been reported previously (Hockett *et al.* 2008). In that study, syringe irrigation was performed using a side-vented needle positioned at 1.5 mm short of WL in canals prepared to size 45, .02 taper (minimally-tapered canals) and to size Protaper F3 (Dentsply Tulsa Dental) with further apical enlargement using a size 35, .02 taper hand instrument (tapered canals). Their results possibly reflect both the ability to mechanically remove microbes in suspension and microbes attached on the canal wall and also the chemical effect of the irrigant, sodium hypochlorite, on the microbes. Therefore, they should be compared with the results of this study regarding both irrigant replacement and wall shear stress. In this study, although irrigant replacement and wall shear stress distribution was overall more favourable in the size 60, .02 taper canal than in the F3 canal (Figs 3 and 4), limited differences could be identified within 1.2 mm apically to the needle tip. Therefore, positioning the needle at 1.5 mm short of WL could in fact lead to a very similar performance. The observed difference could be further reduced if the simulated cases were identical in terms of apical size and root canal taper to the root canals used in the previous study (Hockett *et al.* 2008). Consequently, results of this study are in agreement to the ones reported by Hockett *et al.* (2008).

In another study (Huang *et al.* 2008), it has been reported that less stained collagen was found on the root canal wall in size 20, .08 taper root canals than in size 20, .04 taper following irrigation with a side-vented needle positioned at 4 mm short of WL. This effect was less pronounced and even inverted in certain subgroups, when comparing size 40, .04 taper and 40, .08 taper root canals. According to the authors of that study, the stained collagen was mainly removed by the chemical effect of sodium hypochlorite, although detailed relevant data were not reported. It is possible

that the mechanical effect of the irrigant flow also contributed to the removal of the stained collagen. In this study, an increase in the taper of the root canal always resulted in improved irrigant replacement and wall shear stress distribution apically to the needle tip. Nevertheless, a simultaneous decrease in the maximum wall shear stress near the outlet of the side-vented needle was noted, which could have an effect on the mechanical debridement. It is possible that increasing the apical preparation size or taper of the root canal further than a certain value might in fact decrease the debridement efficacy of irrigation, because the average velocity and the wall shear stress decreases. A similar finding has been reported in a previous study simulating irrigant flow in root canals with different apical sizes (Boutsioukis *et al.* 2010c).

A noteworthy finding of this study was the advantage of the minimally tapered root canal preparation over the tapered ones in terms of irrigant replacement, wall shear stress and apical pressure. It appears that an almost parallel preparation (2% taper) with a large apical size (ISO 60) was the most favourable case. However, this finding should not be directly translated to a clinical suggestion. Improved irrigation efficacy should be collectively evaluated together with resistance to root fracture, possibility of iatrogenic root canal perforation and filling technique requirements prior to deciding the mechanical preparation strategy.

The space available around the needle for reverse flow of the irrigant towards the canal orifice is of critical importance for the overall efficacy of irrigation, as discussed in a previous study (Boutsioukis *et al.* 2010c). An increase in the apical size or taper of the root canal results in an increase in the cross-sectional area of the annulus (the area between two concentric circles) (S) formed between the needle and the root canal wall, according to the equations:

$$S = \pi \frac{D_c^2}{4} - \pi \frac{D_{ext}^2}{4} \quad (1)$$

$$D_c = A + L \cdot T \quad (2)$$

where D_c is the diameter of the root canal at a distance L short of WL, A is the apical size of the root canal, T is the root canal taper and D_{ext} is the external diameter of the needle. The inverse annulus area calculated for the cases studied appeared to be almost proportional to the mean apical pressure (Fig. 5).

Lack of adequate space around the needle and obstruction of the reverse flow led to extremely high pressures in the size 30, .02 taper canal using both needle types. In such a case, the assumptions of a constant flow rate at 0.26 mL s^{-1}, a fixed needle position at 3 mm short of WL and a closed apical foramen would probably fail. Clinically, the operator would be unable either to depress the plunger of the syringe as fast as necessary, or to hold the needle in place. In both cases, the risk of irrigant extrusion would be extremely high. Yet, deviation of the root canal from the perfectly circular cross-section assumed towards an oval cross-section could provide an additional route for the escape of the irrigant.

During irrigation with the side-vented needle positioned at 3 mm short of WL, clinically significant irrigant replacement was limited to 1.5 mm apically to the needle tip in a root canal prepared to a size ProTaper F3 (Dentsply Tulsa Dental) and to 2 mm apically to the needle tip in a minimally tapered root canal (60, .02). This finding augments previous reports on the performance of the side-vented needle (Boutsioukis *et al.* 2010c) suggesting that this type of needle should be positioned within 1 mm short of WL to ensure adequate irrigant replacement in the root canal. The low risk of extrusion, as indicated by the relatively low apical pressures, provides additional support to this suggestion. On the other hand, the flat needle positioned at 3 mm short of WL achieved irrigant replacement almost to the WL in a size 60, .02 taper canal, whilst its performance was slightly less advantageous in the tapered cases studied. It appears that positioning this needle at 2 or 3 mm short of WL can provide effective irrigant replacement and wall shear stress, whilst reducing the risk of extrusion, in agreement to a previous study (Boutsioukis *et al.* 2010c). However, the findings of this study should be further challenged in *ex vivo* and clinical studies to establish a more direct connection with clinical practice.

Conclusions

An increase in the root canal taper was found to improve irrigant replacement and wall shear stress whilst reducing the risk for irrigant extrusion. Irrigant flow in a minimally tapered root canal with a large apical preparation size appeared more advantageous than in the tapered root canals with a smaller apical preparation size.

Acknowledgements

The authors are grateful to B. Benschop for technical assistance. This study was partially funded through a Scholarship for Excellent PhD Students from the

Research Committee of Aristotle University of Thessaloniki, Greece (C.B.) and through Project 07498 of the Dutch Technology Foundation STW (B.V.).

References

Abou-Rass M, Piccinino MV (1982) The effectiveness of four clinical irrigation methods on the removal of root canal debris. *Oral Surgery, Oral Medicine, and Oral Pathology* **54**, 323–8.

Albrecht LJ, Baumgartner JC, Marshall JG (2004) Evaluation of apical debris removal using various sizes and tapers of ProFile GT files. *Journal of Endodontics* **30**, 425–8.

Boutsioukis C, Lambrianidis T, Kastrinakis E, Bekiaroglou P (2007a) Measurement of pressure and flow rates during irrigation of a root canal ex vivo with three endodontic needles. *International Endodontic Journal* **40**, 504–13.

Boutsioukis C, Lambrianidis T, Kastrinakis E (2009) Irrigant flow within a prepared root canal using different flow rates: a Computational Fluid Dynamics study. *International Endodontic Journal* **42**, 144–55.

Boutsioukis C, Verhaagen B, Versluis M, Kastrinakis E, van der Sluis LWM (2010a) Irrigant flow in the root canal: experimental validation of an unsteady Computational Fluid Dynamics model using high-speed imaging. *International Endodontic Journal* **43**, 393–403.

Boutsioukis C, Verhaagen B, Versluis M, Kastrinakis E, Wesselink PR, van der Sluis LWM (2010b) Evaluation of irrigant flow in the root canal using different needle types by an unsteady Computational Fluid Dynamics model. *Journal of Endodontics* **36**, 875–9.

Boutsioukis C, Gogos C, Verhaagen B, Versluis M, Kastrinakis E, van der Sluis LWM (2010c) The effect of preparation size on the irrigant flow in the root canal: evaluation by an unsteady Computational Fluid Dynamics model. *International Endodontic Journal* (In Press).

Chow TW (1983) Mechanical effectiveness of root canal irrigation. *Journal of Endodontics* **9**, 475–9.

Dentsply Tulsa Dental Specialties (2009) Protaper Universal Brochure: The Next Progression in Proficient Performance. https://store.tulsadental.com/lit2/pdfs/ProTaper_Brochurepdf.pdf (Accessed on 23 July, 2009).

Druttman ACS, Stock CJR (1989) An in vitro comparison of ultrasonic and conventional methods of irrigant replacement. *International Endodontic Journal* **22**, 174–8.

Gao Y, Haapasalo M, Shen Y *et al.* (2009) Development and validation of a three-dimensional Computational Fluid Dynamics model of root canal irrigation. *Journal of Endodontics* **35**, 1282–7.

Guerisoli DMZ, Silva RS, Pecora JD (1998) Evaluation of some physico-chemical properties of different concentrations of sodium hypochlorite solutions. *Brazilian Endodontic Journal* **3**, 21–3.

Gulabivala k, Patel B, Evans G, Ng YL (2005) Effects of mechanical and chemical procedures on root canal surfaces. *Endodontic Topics* **10**, 103–22.

Haapasalo M, Endal U, Zandi H, Coil JM (2005) Eradication of endodontic infection by instrumentation and irrigation solutions. *Endodontic Topics* **10**, 77–102.

Hockett JL, Dommisch JK, Johnson JD, Cohenca N (2008) Antimicrobial efficacy of two irrigation techniques in tapered and nontapered canal preparations: an in vitro study. *Journal of Endodontics* **34**, 1374–7.

Hsieh YD, Gau CH, Kung Wu SF, Shen EC, Hsu PW, Fu E (2007) Dynamic recording of irrigating fluid distribution in root canals using thermal image analysis. *International Endodontic Journal* **40**, 11–7.

Huang TY, Gulabivala K, Ng YL (2008) A bio-molecular film ex-vivo model to evaluate the influence of canal dimensions and irrigation variables on the efficacy of irrigation. *International Endodontic Journal* **41**, 60–71.

Kahn FH, Rosenberg PA, Gliksberg J (1995) An in vitro evaluation of the irrigating characteristics of ultrasonic and subsonic handpieces and irrigating needles and probes. *Journal of Endodontics* **21**, 277–80.

Ørstavik D, Qvist V, Stoltze K (2004) A multivariate analysis of the outcome of endodontic treatment. *European Journal of Oral Sciences* **112**, 224–30.

Ram Z (1977) Effectiveness of root canal irrigation. *Oral Surgery, Oral Medicine, and Oral Pathology* **44**, 306–12.

Salzgeber MR, Brilliant DJ (1977) An in vivo evaluation of the penetration of an irrigating solution in root canals. *Journal of Endodontics* **3**, 394–8.

Sedgley CM, Nagel AC, Hall D, Applegate B (2005) Influence of irrigant needle depth in removing bacteria inoculated into instrumented root canals using real-time imaging in vitro. *International Endodontic Journal* **38**, 97–104.

Tilton JN (1999) Fluid and particle dynamics. In: Perry RH, Green DW, Maloney JO, eds. *Perry's Chemical Engineer's Handbook*, 7th edn. New York, USA: McGraw-Hill, pp. 6.1–50.

Zehnder M (2006) Root canal irrigants. *Journal of Endodontics* **32**, 389–98.

